Analysis of Tap-Changer Dynamics and Construction of Voltage Stability Regions

CHEN-CHING LIU AND KHOI T. VU

Abstract—**The destabilizing behavior of on-load tap-changers (OLTC) is an important mechanism responsible for the voltage collapse of interconnected power systems. This paper employs a nonlinear dynamic model of the OLTC, impedance loads, and decoupled reactive power-voltage relations to reconstruct the voltage collapse phenomenon. Trajectories leading to a monotonic fall of bus voltages are obtained from initial conditions outside the stability region of a simple power network. The construction of voltage stability regions is desirable for the prevention of voltage collapse. Based on the proposed M-bus power network model, this research results in (1) a simple criterion for stability of an equilibrium, and (2) a method to obtain a stability region by forming the union of hyperbox subsets of the true region. The theoretical foundations of the proposed method, i.e., characteristics of the equilibria, monotonic behavior of system trajectories, are thoroughly studied.**

I. Introduction

MAJOR POWER system blackouts occurred in France and Belgium in December 1978 and August 1982, respectively [1], [2]. Both events are characterized by a progressive fall of voltages and shortage of reactive power supply. The phenomena of these catastrophic events are now referred to as a "voltage collapse" [3], [4]. A voltage collapse is a slow event relative to the traditional power system machine instability problems. It can occur over a period of minutes to hours, starting with a gradual increase in load demand and decrease in system voltage. Inappropriate control actions due to on-load tap-changers (OLTC's) can aggravate the situation when the system voltage is already low.

Although some theories were proposed to interpret the voltage collapse, there is still no consensus about the mechanisms leading to the problem; a major issue is whether it is a static or dynamic event. A review of the literature is given in the following. Several authors analyzed the phenomena based on the steady-state power network models. Barbier and Barret [1] proposed the calculation of maximal real power transfer over a transmission line and the corresponding voltage level at the load bus. Their main idea is to use the obtained critical voltage as a security limit. Apparently, the reactive power relations are important for the voltage analysis. Carpentier developed a voltage collapse proximity indicator from the optimal power flow calculation [11]. The indicator is defined as the ratio between the incremental reactive power generation and the change in reactive power demand in an area. Galiana [3] proposed the use of feasibility regions, which are defined as the set of all real and reactive power demands for which power flow solutions exist. A measure of the security margin for an operating point inside the feasibility regions is defined. In [5], Kessel and Glavitsch derived a practical security margin for large-scale power systems based on the proximity of an operating point to the boundary of the power flow feasibility region.

At present, the dynamic mechanisms of a voltage collapse are not fully understood. Apparently, the generator excitation, load characteristics are important considerations. The effects of OLTC's were analyzed from the stability point of view by Liu and Wu [6] based on a linearized dynamic tap-changer model, which was proposed by Abe *et al.* [7]. Stability of the discrete model of OLTC's is investigated in [8]. Other works concerning voltage problems of power systems are included as references [9]–[18].

This paper extends the results of [6], [9] in several respects. Since the voltage collapse involves large deviations of system variables, the nonlinear stability techniques are used to analyze the dynamics. In other words, issues on the equilibria and the global stability region are the main concerns here. To reconstruct effects of the OLTC on the collapse phenomena, a simple power system with a single tap-changer is thoroughly analyzed. System trajectories corresponding to a monotonic fall of voltages are obtained from instability of the system.

Based on a general power system model with multiple tap-changers and the reactive power relation of the decoupled power flow equations, qualitative properties of the stable equilibria are derived. It is shown that for a system with M tap-changers, the stable equilibria can exist in only one of the total of 2^M classes of equilibria. This is a partial result of uniqueness of equilibrium for the proposed dynamic model. The proof relies on the monotonic behavior of system trajectories that is characterized in this study.

Manuscript received January 6, 1988; revised August 4, 1988. This work was supported by the National Science Foundation under Grant ECS-86-57671. This paper was recommended by Associate Editor M. Ilic.

The authors are with the Department of Electrical Engineering, University of Washington, Seattle, WA 98195.

IEEE Log Number 8826275.

0098-4094/89/0400-0575$01.00 ©1989 IEEE

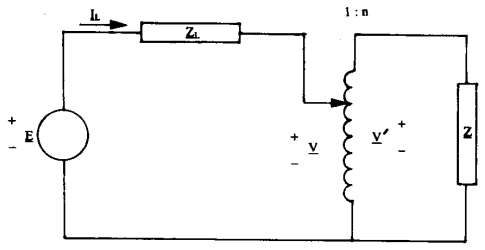

Fig. 1. A simple power system with an OLTC.

Also, this particular class of equilibria is shown to contain the *smallest* equilibrium, which is denoted by α. A simple criterion for stability of α is derived, namely, the Jacobian matrix is *non-singular* at α. For the prevention of voltage collapse, this study results in a method for the construction of a voltage stability region around α, which is formed by union of hyperboxes. The concept of constructing hyperbox approximation of stability or feasibility regions has been used in the literature, e.g., [19]–[21]. The derivation of stability regions using Lyapunov method has been investigated extensively, e.g., [22]. In this study on voltage collapse, our results are derived directly from qualitative behavior of the system trajectories and therefore does not apply Lyapunov method.

The organization of this paper is as follows. Section II presents the dynamic model of the OLTC and the reconstruction of voltage collapse from a simple power system. The general M-bus power system dynamic model is provided in Section III. Section IV describes the stability results, including construction of stability regions.

The notation used in this paper is as follows. In general, boldfaced capital letters are reserved for matrices and boldfaced lowercase letters for vectors. The components of a vector are in subscripted letters, e.g., a_i is the ith component of vector $\boldsymbol{a}$. Inequalities are also used for vectors, e.g., $\boldsymbol{a} \leqslant \boldsymbol{b} (\boldsymbol{a} < \boldsymbol{b})$ means $a_i \leqslant b_i (a_i < b_i)$ for each component i. Complex phasors are denoted by underlined letters.

II. A Reconstruction of Dynamic Voltage Collapse

2.1. A Power System with an OLTC

A simple power system is given in Fig. 1. The purpose of this study is to analyze the effect of OLTC's on system voltages. Therefore, the generator is modeled by a constant voltage source $\underline{E}$. Note that this simplification implies that the generators possess adequate reactive support for the system. The load demand is modeled by an impedance $\underline{Z}$. For the dynamic study, a more complete load model would incorporate real and reactive power demands which vary with the system frequency and bus voltages [25]. For a study on the voltage behavior, the constant complex power load model usually adopted in a power flow study is not appropriate. Also for the purpose of the analysis in this section, the transmission line is modeled by an impedance $\underline{Z}_L$. For the general case, which will be treated in Sections III and IV, the π-equivalent line models are incorporated.

The OLTC's are used to regulate the load voltage magnitude. In the case of Fig. 1, the secondary voltage magnitude V' would be regulated at a reference value V_o. In an actual OLTC, the taps are discrete. However, in practice, a step in the tap position contributes a relatively small amount of voltage correction, e.g., 0.625 percent (1/8 of 5 percent) of the nominal voltage. In a recent numerical study [26], it is concluded that the rounding of transformer taps to their nearest discrete values is practically acceptable. Therefore, in this study the following continuous model [7] is adopted.

$$\frac{dn}{dt} = \frac{1}{T}(V_o - V') \tag{1}$$

where n is the turn ratio, V' and V_o are the secondary voltage measurement and reference voltage, respectively, and T is the time constant of the OLTC.

2.2. Dynamic Equation

In the case of Fig. 1, the network is assumed to be in a sinusoidal steady state, and the network relationship is given by

$$\underline{E} = \underline{Z}_L \underline{I}_L + \underline{V}. \tag{2}$$

Also, it is easy to see that the load voltage

$$\underline{V}' = \frac{\underline{E}}{\underline{Z}_L + \underline{Z}/n^2} \frac{\underline{Z}}{n} = \frac{n\underline{E}\underline{Z}}{n^2\underline{Z}_L + \underline{Z}}. \tag{3}$$

Based on (1) and (3) the system equation can be obtained as

$$\frac{dn}{dt} = \frac{1}{T}\left(V_o - \frac{nEZ}{\left[n^4 Z_L^2 + 2n^2 Z Z_L \cos(\theta_L - \theta) + Z^2\right]^{1/2}}\right) \tag{4}$$

where $\underline{Z}_L = Z_L \angle \theta_L$ and $\underline{Z} = Z \angle \theta$.

Since the model of (4) is nonlinear, a systematic approach to the stability analysis would follow the steps of calculating the equilibrium points, analyzing the local (linearized) stability, and determining the region of attraction for the stable equilibrium. In [9], the single OLTC system is analyzed by this approach. The result on local stability provided in [6] was used in the derivation. In this paper, only a qualitative interpretation of the voltage collapse is provided. The reader is referred to [9] for proofs.

2.3. Equilibrium

For convenience, the equilibrium points of (4), solutions of $dn/dt = 0$, are given here. It is noted that the system

described by (4) has at most two equilibria, i.e.,

$$n_{1o}=\sqrt{\frac{E^2Z^2-2V_o^2ZZ_L\cos(\theta_L-\theta)-\sqrt{\left[E^2Z^2-2V_o^2ZZ_L\cos(\theta_L-\theta)\right]^2-4Z^2Z_L^2V_o^4}}{2Z_L^2V_o^2}} \tag{5}$$

$$n_{2o}=\sqrt{\frac{E^2Z^2-2V_o^2ZZ_L\cos(\theta_L-\theta)+\sqrt{\left[E^2Z^2-2V_o^2ZZ_L\cos(\theta_L-\theta)\right]^2-4Z^2Z_L^2V_o^4}}{2Z_L^2V_o^2}}. \tag{6}$$

For this study only real, positive solutions of n_{1o}, n_{2o} are of interest. From (5), this requires the condition

$$\left(E^2Z^2-2V_o^2ZZ_L\cos(\theta_L-\theta)\right)^2\geq 4Z_2Z_L^2V_o^4. \tag{7}$$

To guarantee the above condition to hold for all possible load power factor angles $\theta, 0\leq\theta\leq\pi/2$ the following assumption will be made.

$$E^2Z>4Z_LV_o^2 \tag{A1}$$

It is easy to show that if assumption (A1) holds, then the condition of (7) is true regardless of whether the load is inductive, resistive, or capacitive. As a result, the system of (4) will have two real positive equilibria, say n_{1o} and n_{2o}, where $n_{1o}<n_{2o}$. The inequality of (A1) is not restrictive from a practical point of view. Normally the load impedance Z would be much greater than the line impedance Z_L.

2.4. *Stability Analysis*

As indicated earlier, this section will emphasize the physical interpretation of the voltage collapse mechanism due to an OLTC. Therefore, only the qualitative explanation will be given. Referring to (4), it is straightforward to plot the right hand side as a function of the tap ratio n. The plots of dn/dt and V' (the second term in the parentheses of (4)) are presented in Fig. 2(a) and 2(b).

Based on the sign of dn/dt in the intervals of $(0, n_{1o})$, (n_{1o}, n_{2o}) and (n_{2o}, ∞), the dynamic behavior of the tap changer can be described by the curve of Fig. 2(c). In other words, if the initial position of the tap falls within $(0, n_{2o})$, then the trajectory of (4) will converge to n_{1o}, which indeed is the stable equilibrium.

On the other hand, in case the initial value $n(0)$ of the tap position falls beyond n_{2o}, then, according to Fig. 2(a), $dn/dt>0$, and, therefore, n will increase monotonically. The curve of Fig. 2(b) then shows that the load voltage V' will also decrease monotonically. Without restriction on the maximally allowable tap position, the load voltage V' would approach zero! The voltage behavior for the interval (n_{2o}, ∞) provides an analytical interpretation for the accentuating voltage drop during a voltage collapse [1].

Practically, the tap position would reach the highest possible ratio, $n_{\max}$, and stay at that position. In this case the dynamics of the OLTC will no longer affect the system voltage. Other mechanisms of voltage collapse may cause the system voltage to deteriorate; for example, other OLTC's, generator excitation, line switching, switched capacitors, etc.

A comparison between the behaviors of the discrete and continuous tap-changer models is made here. The dynamics of an OLTC can be represented by the discrete model [8]

$$\Delta n=f(-V'+V_o)$$

where V' is the load voltage magnitude as shown in Fig. 1, V_o is the reference, and f is defined by

$$f(x)=\begin{cases}1, & \text{if } x>\varepsilon\\ 0, & |x|\leq\varepsilon\\ -1, & x<-\varepsilon.\end{cases}$$

It is assumed here that, as in [8], a one-step change in the tap-ratio results in a voltage deviation less than 2ε. This is to prevent oscillation between tap positions.

Equilibrium is attained when $|-V'+V_o|\leq\varepsilon$. Note that, under Assumption (A1), the equation $-V'(n)+V_o=0$ has two (real) solutions n_{1o} and n_{2o}, as given by (5)–(6). However, these values of n_{1o} and n_{2o} may not be physically meaningful in the discrete model. In this case the actual equilibrium positions should lie beside n_{1o} and n_{2o} in such a way that the resulting voltages deviate from V_o by no more than ε. Without loss of rigor, it can be assumed that within ε of the voltage reference V_o, there is a unique equilibrium e_1 close to n_{1o}, and similarly e_2 close to n_{2o}.

Depending on the values of n, there are two cases:

(1) $e_1<n<e_2$: In this case, the corresponding voltage V' is higher than V_o by more than ε. Therefore, n tends to decrease until e_1 is reached, as shown in Fig. 2(d).

(2) $0<n<e_1$, or $n>e_2$: If this is the case, the tap position increases as time go on. For $n>e_2$, this tendency implies a monotonic fall of load voltage.

The similarity of the dynamic behavior predicted by the continuous and discrete models can be seen by comparing Fig. 2(c) and (d). For a general power system, the comparison between the dynamic behaviors of the two models is yet to be investigated.

The approach developed in this section can be generalized to the M-bus power systems. In the next section, the general case will be discussed. The analysis will start by finding the equilibrium points of the dynamic model. The state space of tap positions will be partitioned into stable or unstable regions, each corresponding to some equilibria. This is illustrated in Fig. 2(c) for the simple power system. Also note that each of the three regions in Fig. 2(c) is invariant in the sense that a trajectory will not cross an

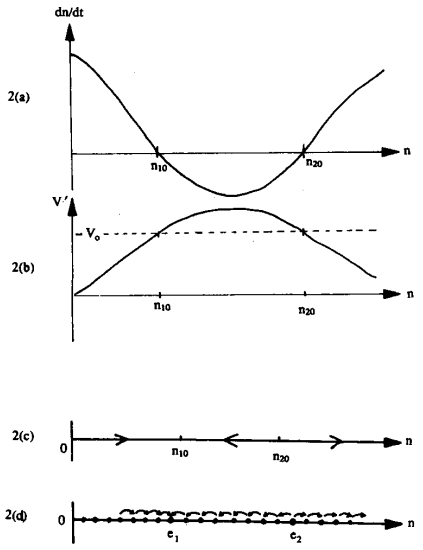

Fig. 2. Plots of dn/dt, load voltage V', and "potential energy" versus tap-ratio n for the simple power system.

equilibrium to reach another segment of n. This is due to the monotonic behavior of first-order differential systems.

There are major differences between the simple and the general cases. The latter case deals with much greater complexity in mathematical analysis. Explicit calculation of the *exact* stability region for the general case would be extremely difficult, if possible at all.

III. Dynamic Power Network Model— M OLTC Case

Referring to the M-tap-changer model in Fig. 3, the notation will be defined below.

- M number of OLTC's buses (i.e., nodes). These buses are numbered *from 1 to M*.
- N number of intermediate buses that are neither OLTC nor generator buses. These buses are numbered *from M + 1 to M + N*.
- r number of generator buses. These buses are numbered *from M + N + 1 to M + N + r*.
- n_i tap ratio of OLTC i, $i=1,2,\cdots,M$.
- T_i time constant associated with OLTC i, $i=1,2,\cdots M$.
- $\underline{V}_{io}$ nominal voltage of the secondary side of OLTC i, $i=1,2,\cdots,M$.
- $\underline{V}_i$ voltage at bus i, $i=1,2,\cdots,M+N+r$.
- V_i' voltage on secondary side of OLTC i, $i=1,2,\cdots,M$.
- b_{ii} self-susceptance at bus i, $i=1,2,\cdots,M+N+r$. Note that $b_{ii}>0$
- b_{ik} mutual susceptance between bus i and bus k, where $i,\ k=1,2,\cdots,M+N+r$ and $i\neq k$. Note that $b_{ik}\geqslant 0$. It is assumed that $b_{ik}=b_{ki}$, i.e., no phase shifting transformers.

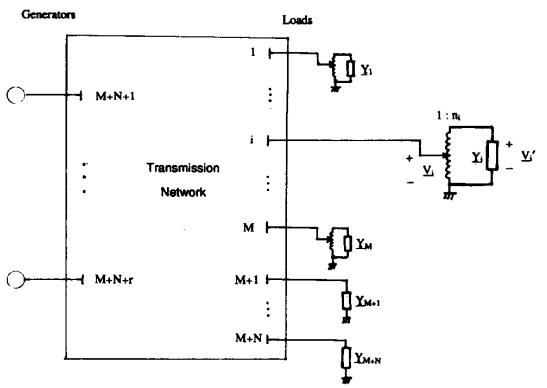

Fig. 3. Power network model for the case of M OLTC's.

- $\underline{Y}_i$ admittance of the load connected to OLTC i, $i=1,2,\cdots,M$.

In the analysis that follows, it will be assumed that the loads are complex admittances Y_i, but inductive in nature, i.e., $y_i=\mathrm{Im}\{\underline{Y}_i\}>0$, which is normally the case in a power system. To model the reactive power and voltage relation the so-called *decoupled power flow equations* are used. The power system network under consideration is interconnected.

For each load bus i, $i=1,2,\cdots,M$, the dynamic equation is

$$\frac{dn_i}{dt}=\frac{1}{T_i}(V_{io}-V_i') \tag{8}$$

and the *decoupled power flow equation* is

$$V_i^2 b_{ii}-\sum_{k=1,\,k\neq i}^{M+N+r} V_i V_k b_{ik}=-V_i'^2 y_i \tag{9}$$

where the shunt susceptances of the π-equivalents of transmission lines are included in the b_{ii}.

Replacing $V_i'=n_i V_i$ in (8), one obtains

$$\frac{dn_i}{dt}=\frac{1}{T_i}(V_{io}-n_i V_i). \tag{10}$$

Substituting $V_i'=n_i V_i$ into (9) and manipulating the resultant equation, it can be shown that

$$V_i\left(b_{ii}+n_i^2 y_i\right)-\sum_{k=1,\,k\neq i}^{M} V_k b_{ik}-\sum_{k=M+1}^{M+N} V_k b_{ik}-\sum_{k=M+N+1}^{M+N+r} V_k b_{ik}=0. \tag{11}$$

Since generators are treated as perfect voltage sources in this study, $V_k=$ constant for each $k=M+N+1,\cdots,M+N+r$; thus the last term on the LHS of (11) is a constant for each i. Equation (11) can be written as follows:

$$V_i\left(b_{ii}+x_i^2\right)-\sum_{k=1,\,k\neq i}^{M} V_k b_{ik}-\sum_{k=M+1}^{M+N} V_k b_{ik}=q_i \tag{12}$$

where

$$q_i := \sum_{k=M+N+1}^{M+N+r} V_k b_{ik} \tag{13}$$

and

$$x_i := n_i \sqrt{y_i}\,. \tag{14}$$

Note that the assumption of $y_i > 0$ makes the change of variable in (14) possible. In the proposed model, each load bus i, $i = 1, \cdots, M$ is represented by a dynamic equation (10) and an algebraic equation (12).

For each intermediate bus j, $j = M+1, \cdots, M+N$, the corresponding *decoupled power flow equation* is given by

$$V_j^2 b_{jj} - \sum_{k=1,\, k\neq j}^{M+N+r} V_j V_k b_{jk} = 0 \tag{15}$$

which can be rearranged to yield

$$V_j b_{jj} - \sum_{k=1}^{M} V_k b_{jk} - \sum_{k=M+1,\, k\neq j}^{M+N} V_k b_{jk} = q_j \tag{16}$$

where

$$q_j := \sum_{k=M+N+1}^{M+N+r} V_k b_{jk} \tag{17}$$

To obtain a state-space dynamic representation in state variables x_i, $i = 1, \cdots, M$ the algebraic constraints of (12) and (16) will be eliminated. This is possible because one can solve for the voltages $V_1, \cdots, V_M$ explicitly from these equations and substitute them into (10). An outline of the above process is presented below.

Putting (12) and (16) together, a linear matrix equation can be obtained, i.e.,

$$\boldsymbol{X}\boldsymbol{v} = \boldsymbol{q} \tag{18}$$

where

$$\boldsymbol{v} = (V_1, \cdots, V_M, V_{M+1}, \cdots, V_{M+N})^T$$

$$\boldsymbol{X} = \left[\begin{array}{cccc|ccc} x_1^2 + b_{11} & \cdots & & -b_{1M} & -b_{1,M+1} & \cdots & -b_{1,M+N} \\ -b_{21} & x_2^2 + b_{22} & \cdots & -b_{2M} & -b_{2,M+1} & \cdots & -b_{2,M+N} \\ \vdots & \vdots & \ddots & \vdots & \vdots & & \vdots \\ -b_{M1} & -b_{M2} & \cdots & x_M^2 + b_{MM} & -b_{M,M+1} & \cdots & -b_{M,M+N} \\ \hline -b_{M+1,1} & -b_{M+1,2} & \cdots & -b_{M+1,M} & b_{M+1,M+1} & \cdots & -b_{M+1,M+N} \\ \vdots & \vdots & & & & \ddots & \vdots \\ -b_{M+N,1} & -b_{M+N,2} & & & & & b_{M+N,M+N} \end{array}\right] \tag{19}$$

and $\boldsymbol{q}$ is a vector of size $M+N$ whose components are defined by (13) or (17). To obtain a set of dynamical equations, (18) needs to be solved for $V_1, V_2, \cdots, V_M$ and the result is then plugged into (10). Cramer's rule gives for each i, $i = 1, 2, \cdots, M$,

$$V_i = \sum_{j=1}^{M+N} \frac{X_{ij}}{\det \boldsymbol{X}}\, q_j \tag{20}$$

where X_{ij} is the ij cofactor of the *symmetric* matrix $\boldsymbol{X}$. Substituting (14) and (20) into (10), the following set of M dynamical equations results:

$$\frac{dx_i}{dt} = \frac{1}{T_i}\left(\sqrt{\bar{y}_i} V_{io} - \frac{x_i}{\det \boldsymbol{X}} \sum_{j=1}^{M+N} X_{ij} q_j\right) \tag{21}$$

for $i = 1, 2, \cdots, M$. Note that (21) represents a nonlinear dynamic system in the state space.

Remarks:

1) The generator rotor and excitation system dynamics are ignored in the proposed model. The assumption of constant voltage source implies that the generators can provide the necessary amount of reactive power and that the exciter response is fast enough. For a more realistic model, if a maximum Var limit is reached, one may be able to model the corresponding bus as a PQ-bus, or perhaps the dynamics of exciters and field windings should be added [27]. At present, it is not clear whether the rotor dynmaics play a key role in a voltage collapse. Reference [10] presents a linearized analysis of the effects of reactive power/voltages on the rotor stability.

2) At this point, a general load model for the voltage collapse analysis is not available. The familiar constant-PQ load model for power flow studies is clearly inadequate since bus voltages are sensitive to reactive power injections. A mechanism of collapse due to induction motor dynamics is proposed in [28]. In the future, various mechanisms such as tap-changers and unduction motors should be combined to achieve a more complete load model.

3) The decoupled power flow model (9), is an approximation of the full load flow model which is valid when line angles and line (real power) losses are small. The real power relations may also be important, since the voltage collapse may occur when a maximal *real* power limit is exceeded [1]. this paper is concentrated on the effects of the OLTC's. It is believed that the $Q-V$ relation of (9) serves as a reasonable nonlinear approximation of the steady state power system as far as the voltage behavior is concerned. It is further pointed out that, for the one tap-changer case, as one varies the impedance angle of the load, (6), results in the smallest value when the impedance is purely inductive. This implies that the stability region $(0, n_{20})$ is the smallest, i.e., the worst case of the tap-changer effect is being analyzed when a purely reactive load is considered. ◆

IV. Dynamic Analysis of M OLTC Case

In this section, the stability analysis will be treated for the general case, for which M OLTC's are involved. It is shown that at most one class of equilibria out of 2^M classes can contain a stable equilibrium. This class contains the *smallest* equilibrium α (i.e., there is an equilibrium α with $\alpha < e$ for all other equilibria e), whose stability is guaranteed if the associated Jacobian matrix is *non-singular*. Furthermore, a method is developed for the construction of stability region in terms of hyperboxes for the above-mentioned equilibrium.

4.1. Characterization of Equilibria

The equilibria of (21) can be obtained from roots of the system of nonlinear algebraic equations $dx_i/dt = 0$, $i = 1,2,\cdots, M$, i.e., they belong to the set

$$\Im = \left\{ x_o \in \boldsymbol{R}^M : \left.\frac{dx_i}{dt}\right|_{x=x_0} = 0, \quad i = 1,2,\cdots, M \right\}. \quad (22)$$

From (21) the set of points satisfying $dx_i/dt = 0$ for a particular i is represented by the following equation:

$$0 = x_i^2[\sqrt{y_i} V_{io} X_{ii}] - x_i \left[\sum_{j=1}^{M+N} X_{ij} q_j \right] + \sqrt{y_i} V_{io} \left(b_{ii} X_{ii} + \sum_{k=1,\, k\neq i}^{M+N} - b_{ik} X_{ik} \right) \quad (23)$$

which is quadratic in x_i with coefficients in terms of $x_1,\cdots, x_{i-1}, x_{i+1},\cdots, x_M$. As a remark, although the M nonlinear algebraic equations (23) take the form of polynomials, there is no guarantee that the number of solutions is finite.

From (23) for a given $(x_1,\cdots, x_{i-1}, x_{i+1},\cdots, x_M)$, $dx_i/dt = 0$ has at most two *real* solutions which can be denoted implicitly as

$$x_i = L_i(x_1,\cdots, x_{i-1}, x_{i+1},\cdots, x_M) \quad (24)$$

and

$$x_i = H_i(x_1,\cdots, x_{i-1}, x_{i+1},\cdots, x_M) \quad (25)$$

where L_i and H_i are real-valued functions defined on a certain subset of $\boldsymbol{R}^{M-1}$ and $L_i \leqslant H_i$. (The names L and H refer to "*L*ower" and "*H*igher" real solutions (if exist), respectively, of a quadratic equation.)

Since for each i, either (24) or (25) must hold for an equilibrium point, the intersection of either $x_i = L_i(x_1,\cdots, x_{i-1}, x_{i+1},\cdots, x_M)$ or $x_i = H_i(x_1,\cdots, x_{i-1}, x_{i+1},\cdots, x_M)$, $i = 1,\cdots, M$, forms a class of equilibria. Hence, the maximally possible number of equilibrium classes would be 2^M. In this subsection, it will be shown that the class for which $x_i = L_i(x_1,\cdots, x_{i-1}, x_{i+1},\cdots, x_M)$ for all i, $i = 1,\cdots, M$, may yield a stable equilibrium and all other classes can only contribute unstable equilibria. Even if the total number of equilibria is finite, there is no guarantee that each class has no more than one equilibrium. In fact, an example in the case of 2 OLTC's was found for which the class determined by $x_1 = L_1(x_2)$ and $x_2 = L_2(x_1)$ yields *two* equilibria (see Appendix 1).

To examine the stability characteristic of a given equilibrium, geometric properties of the "surfaces" L_i and H_i will be examined. First the domain of these functions is characterized.

Lemma 1:

(1) For each $i = 1,\cdots, M$, the functions L_i and H_i of $M-1$ variables are well-defined over the following subset of $\boldsymbol{R}^{M-1}$:

$$\left\{ (x_1,\cdots, x_{i-1}, x_{i+1},\cdots, x_M) \,|\, y_i \geqslant \frac{\left[\sum_{j=1}^{M+N} X_{ij} q_j \right]^2}{4V_{io}^2 X_{ii} \left[b_{ii} X_{ii} + \sum_{k=1,\, k\neq i}^{M+N} - b_{ik} X_{ik} \right]} \right\} \quad (26)$$

where X_{ij} is the ij-cofactor of $\boldsymbol{X}$.

(2) The domain defined in (26) occupies the whole space if and only if

$$y_i \leqslant \frac{q_i^2}{4V_{io}^2 b_{ii}} \quad (27)$$

where q_i is given in (13).

(3) If the functions L_i and H_i are defined at $\boldsymbol{b} \in \boldsymbol{R}^{M-1}$ then they are defined for all $\boldsymbol{a} \leqslant \boldsymbol{b}$. #

Proof: Recall that (23) must be satisfied by any equilibrium for all $i = 1,2,\cdots, M$. Since (23) is a quadratic equation in x_i, the necessary and sufficient condition for (23) to have roots (or in other words, for which L_i and H_i to be well defined) is that the discriminant is nonnegative, i.e.,

$$0 \leqslant \left[\sum_{j=1}^{M+N} X_{ij} q_j \right]^2 - 4 y_i V_{io}^2 X_{ii} \left[b_{ii} X_{ii} + \sum_{k=1,\, k\neq i}^{M+N} - b_{ik} X_{ik} \right] \quad (28)$$

$$\Leftrightarrow y_i \leqslant \frac{\left[\sum_{j=1}^{M+N} X_{ij} q_j \right]^2}{4V_{io}^2 X_{ii} \left[b_{ii} X_{ii} + \sum_{k=1,\, k\neq i}^{M+N} - b_{ik} X_{ik} \right]}. \quad (29)$$

The RHS of (29) is independent of y_i and has the form $g_i(\cdot)/4V_{io}^2$ where $g_i(\cdot)$ is defined in Appendix 4. There it is shown that the infimum of the RHS of (29) over $\boldsymbol{R}^{M-1}$ is $q_i^2/(4V_{io}^2 b_{ii})$. This proves (27). Also, since the RHS of (29) is strictly decreasing (Appendix 4), if (29) is satisfied by $\boldsymbol{b}$ it is also satisfied for all $\boldsymbol{a} \leqslant \boldsymbol{b}$. Thus (3) follows. ◆

Note that since tap-ratios are assumed to be non-negative, only the first-quadrant portion of the domain is of concern here. Also, unless (27) is satisfied for each i, care

should be taken when dealing with these L- and H-functions. Practically, the condition of (27) may not be satisfied. Consider the case when an OLTC is not connected to any generator. Then the mutual susceptance $b_{ik} = 0$ for all k, $k = M+N+1, \cdots, M+N+r$. Hence q_i would be 0 from its definition in (13). Since $y_i > 0$ by assumption and $q_i = 0$, (27) cannot be satisfied. Consequently, the domain of L- and H-functions is restricted to a bounded region in $\boldsymbol{R}^{M-1}$, given by (26).

The relation between dx_i/dt and the surfaces $L_i(\cdot)$, $H_i(\cdot)$ is summarized in the following.

Property 1:

(a) For each i, $i = 1, \cdots, M$, L_i and H_i are positive.

(b) Wherever L_i and H_i are defined,

$$dx_i/dt < 0 \Leftrightarrow L_i(x_1, \cdots, x_{i-1}, x_{i+1}, \cdots, x_M) < x_i < H_i(x_1, \cdots, x_{i-1}, x_{i+1}, \cdots, x_M).$$

(c) $dx_i/dt > 0$ at points outside the set defined in (26). #

Proof: Note that $dx_i/dt = 0$ is equivalent to (23) which takes the form

$$ax_i^2 - bx_i + c = 0$$

where a, b and c are positive. Since $x_i = L_i(\cdot)$ and $x_i = H_i(\cdot)$ are solutions, $L_i \cdot H_i = c/a$ and $L_i + H_i = b/a$. Therefore, both L_i and H_i are positive whenever they are defined. Also, since the sign of dx_i/dt is the same as that of $ax_i^2 - bx_i + c = a(x_i - L_i(\cdot))(x_i - H_i(\cdot))$, condition (b) is true. Condition (c) follows from the fact that when $ax_i^2 - bx_i + c$ has no roots, it has the same sign as the leading coefficient a. ◆

In other words, Property 1 asserts that the surfaces defined by $x_i = L_i(\cdot)$ and $x_i = H_i(\cdot)$ lie in the first quadrant of $\boldsymbol{R}^M$, and divide this quadrant into 3 different regions: the region sandwiched by the surfaces corresponding to $dx_i/dt < 0$, the surfaces given by $dx_i/dt = 0$, and the remaining region, which satisfies $dx_i/dt > 0$.

An important characteristic of the L_i and H_i functions, namely monotonicity, is presented in the following lemma.

Lemma 2: For each $i = 1, 2, \cdots, M$, the function L_i is strictly increasing, the function H_i is strictly decreasing over their domains. #

Proof: See Appendix 5. ◆

An illustration of L- and H-functions for the case of 2 tap-changers is shown in Fig. 4. Note that each function is monotonic over the appropriate domain.

In the stability analysis, invariant sets are of importance; they are closely related to the characteristics of equilibria. Two invariant sets are exhibited in the following lemma.

Lemma 3:

The sets **N** and **P** defined by

$$\mathbf{N} = \{ \boldsymbol{x} \in \boldsymbol{R}^M | dx_i/dt \leqslant 0 \text{ for } i = 1, \cdots, M \}$$

$$\mathbf{P} = \{ \boldsymbol{x} \in \boldsymbol{R}^M | dx_i/dt \geqslant 0 \text{ for } i = 1, \cdots, M \} \quad (30)$$

are invariant sets of the dynamic system defined by (21). #

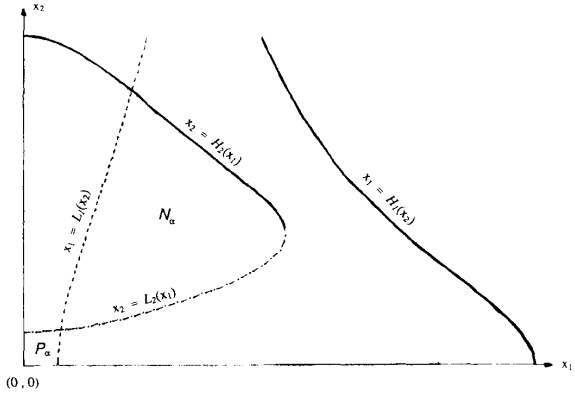

Fig. 4. L- and H-functions for 2 tap-changers.

Proof: See Appendix 6. ◆

Based on Lemmas 2 and 3, one can judge the instability of almost all classes of equilibria. This is stated in the following Proposition.

Proposition 1: Stable equilibria must be contained in the intersection of the surfaces L_i, $i = 1, 2, \cdots, M$. #

Proof: See appendix 7. ◆

For convenience, the class of equilibria associated with the surfaces L_i, $i = 1, 2, \cdots, M$, is denoted by **L**. In the remaining of this subsection, it is shown that the class **L** contains the *smallest* equilibrium, i.e., the one with smallest coordinates (infimum) in every dimension. The following definition greatly simplifies the future developments of this section.

Definition:

$\{\boldsymbol{a}_k, k = 0, 1, \cdots\}$ is the L-sequence starting at $\boldsymbol{x}$ if

(1) $L_i(x_1, \cdots, x_{i-1}, x_{i+1}, \cdots, x_M)$ exists for each i, $i = 1, \cdots, M$.

(2) $\boldsymbol{a}_o = \boldsymbol{x}$.

(3) $\boldsymbol{a}_{k+1}$ is defined recursively as follows:

$$(\boldsymbol{a}_{k+1})_i = L_i((\boldsymbol{a}_k)_1, \cdots, (\boldsymbol{a}_k)_{i-1}, (\boldsymbol{a}_k)_{i+1}, \cdots, (\boldsymbol{a}_k)_M), \quad i = 1, \cdots, M. \quad \#$$

In other words, starting at $\boldsymbol{a}_o$, one takes the projection of $\boldsymbol{a}_o$ onto each surface L_i, $i = 1, \cdots, M$, to get the ith component $(\boldsymbol{a}_1)_i$ of $\boldsymbol{a}_1$. The process repeats with $\boldsymbol{a}_1$ and so on. Note that according to this definition, an L-sequence need not have an infinite number of elements, which is the case when at some iteration k, the projection ceases to exist because the exterior of the domains of L_i's is reached. Suppose an L-sequence has infinitely many elements, its convergence is guaranteed by the following lemma.

Lemma 4: The following statements are true for the L-sequence starting at $\boldsymbol{x}$:

(1) If $x_i \geqslant L_i(x_1, \cdots, x_{i-1}, x_{i+1}, \cdots, x_M)$, $\forall i$, $i = 1, \cdots, M$, with at least one strict inequality then the L-sequence starting at $\boldsymbol{x}$ converges (decreasingly) to $\boldsymbol{a} \in \mathbf{L}$ and $\boldsymbol{a} < \boldsymbol{x}$.

(2) If $x_i \leqslant L_i(x_1, \cdots, x_{i-1}, x_{i+1}, \cdots, x_M)$, $\forall i$, $i = 1, \cdots, M$ (with at least one strict inequality), and if there is

$\boldsymbol{b} \in \mathbf{L}$ such that $\boldsymbol{x} \leqslant \boldsymbol{b}$ then the L-sequence starting at $\boldsymbol{x}$ converges (increasingly) to some $\boldsymbol{a} \in \mathbf{L}$ and $\boldsymbol{x} < \boldsymbol{a} \leqslant \boldsymbol{b}$. #

Proof: See Appendix 8. ◆

Remark: The existence of $\boldsymbol{b}$ in (2) of Lemma 4 is important to guarantee that the exterior of the domains of L_i's is never reached.

In the following Proposition, the class $\mathbf{L}$ is shown to contain the smallest equilibrium denoted by α. Note that α_i, the ith component of α, is defined to be the infimum over all points in $\mathbf{N}$. It will be shown that α is an equilibrium in $\mathbf{L}$.

Proposition 2:

Assume that the set $\mathbf{N}$ as defined in (30) is non-empty. Then $\mathbf{N}$ has the smallest element α, i.e., $\alpha < x$, $\forall x \in \mathbf{N}$ and $x \neq \alpha$. Furthermore, $\alpha \in \mathbf{L}$. #

Proof: Assume that $\mathbf{N} \neq \emptyset$. Define α as follows:

$$\alpha_i = \inf\{x_i\colon x \in \mathbf{N}\}, \qquad \text{for } i = 1, \cdots, M.$$

Note that α is well-defined since for each component i, $\{x_i\colon x \in \mathbf{N}\}$ is non-empty and bounded from below (by 0). It shall be shown that $\alpha \in \mathbf{L}$ (hence, $\alpha \in \mathbf{N}$).

Given an $\epsilon > 0$ arbitrary. For each i, $i = 1, \cdots, M$, there is $x \in \mathbf{N}$ so that $\alpha_i + \epsilon > x_i \geqslant L_i(x_1, \cdots, x_{i-1}, x_{i+1}, \cdots, x_M) \geqslant L_i(\alpha_1, \cdots, \alpha_{i-1}, \alpha_{i+1}, \cdots, \alpha_M)$ where the first inequality is due to the property of infimum, the second to the fact that $x \in \mathbf{N}$, and the third to monotonicity of L_i.

Thus $\alpha_i \geqslant L_i(\alpha_1, \cdots, \alpha_{i-1}, \alpha_{i+1}, \cdots, \alpha_M)$ for $i = 1, \cdots, M$. By contradiction, assume strict inequality holds for some i then from (1) of Lemma 4, the L-sequence starting at α converges (decreasingly) to an equilibrium $e, e < \alpha$. But $e \in \mathbf{N}$, a contradiction follows. Therefore, $\alpha_i = L_i(\alpha_1, \cdots, \alpha_{i-1}, \alpha_{i+1}, \cdots, \alpha_M)$ for $i = 1, \cdots, M$. In other words $\alpha \in \mathbf{L}$.

From the definition of $\alpha, \alpha \leqslant x, \forall x \in \mathbf{N}$. It remains to show that $x > \alpha$, $\forall x \in \mathbf{N} - \{\alpha\}$. Let $x \in \mathbf{N} - \{\alpha\}$, then $\alpha \leqslant x$ with $\alpha_j < x_j$ for some component j. For $i \neq j$,

$$\alpha_i = L_i(\alpha_1, \cdots, \alpha_{i-1}, \alpha_{i+1}, \cdots, \alpha_M) < L_i(x_1, \cdots, x_{i-1}, x_{i+1}, \cdots, x_M) \leqslant x_i$$

which implies that $\alpha < x$. ◆

Remarks:

1) For the case of two tap-changers (i.e., $M = 2$) in Fig. 4, α is the intersection of $x_1 = L_1(x_2)$ and $x_2 = L_2(x_1)$.

2) The "infimum" α defined in Proposition 2 is the limit of the L-sequence starting at $\mathbf{0}$. This follows from the second statement of Lemma 4.

3) In the general case, α is the point around which a stability region will be constructed.

4.2. Construction of Stability Regions

The use of a voltage stability region for on-line operation is explained here. As the system equilibrium is perturbed, say, due to generator tripping or load shedding, the post-disturbance equilibrium and the stability region will both vary. If the initial tap positions of the post disturbance system fall outside the stability region, a voltage collapse would occur. From the operational point of view, it is desirable to lock the relevant tap positions in order to prevent further aggravation in the system voltage.

In this subsection, it is shown that (1) this smallest equilibrium α is asymptotically stable if the associated Jacobian matrix is *non-singular*, and (2) a method to construct a stability region in terms of hyperboxes is proposed.

Lemma 5:

The set $\mathbf{P}_\alpha = \{w\colon \mathbf{0} \leqslant w \leqslant \alpha\} \cap \{w\colon dx/dt(x = w) \geqslant \mathbf{0}\}$ is an invariant set of the dynamical equations (21) and each trajectory in $\mathbf{P}_\alpha$ converges (increasingly) to α. #

Proof: See Appendix 9. ◆

Using the case of two tap-changers (Fig. 4) as an example, the set $\mathbf{P}_\alpha$ is the region surrounded by the curves $x_1 = L_1(x_2)$, $x_2 = L_2(x_1)$ and the x_1-, x_2- axes.

The asymptotic stability of α is established in the following lemma.

Lemma 6:

Suppose that the set

$$\mathbf{N}_\alpha = \{z\colon z \in \mathbf{N} - \{\alpha\}, \text{ and there is no equilibrium } e \text{ with } \alpha < e \leqslant z\} \quad (31)$$

is non-empty. Then for each $w \in \mathbf{P}_\alpha$, $z \in \mathbf{N}_\alpha$, the hyperbox $\{x\colon w \leqslant x \leqslant z\}$, is a region of attraction. As a result, α is asymptotically stable. #

Proof: See Appendix 10. ◆

Note that the set $\mathbf{N}_\alpha$ in Fig. 4 is enclosed by the curves $x_1 = L_1(x_2)$, $x_2 = L_2(x_1)$ and $x_2 = H_2(x_1)$.

According to Lemma 5, a region containing trajectories that converge *increasingly* to α always exist. Lemma 6 states that, in addition, there is a region containing trajectories that converge *decreasingly* to α and that α is asymptotically stable. When the conditions of Lemma 6 are satisfied, regions of attraction can be approximated by hyperboxes. Naturally, the union of all such hyperboxes is also a region of attraction. Since $\mathbf{0}$ can always be taken as the "lowest" vertex of the hyperbox, one arrives at the following Proposition.

Proposition 3:

Assume that the set $\mathbf{N}_\alpha$ as defined in (31) is non-empty then α is asymptotically stable and the union

$$A = \bigcup_{z \in \mathbf{N}_\alpha} \{x\colon \mathbf{0} \leqslant x \leqslant z\}$$

is a region of attraction of α. #

To construct a hyperbox, two vertices need to be found. As mentioned previously, the origin can always serve as the lower one. The upper vertex can be any point from $\mathbf{N}_\alpha$ with all negative or zero derivatives. If the location of α is known, one can choose a point z with coordinates larger than α in all dimensions. From Lemma 6, it is necessary to ensure that no equilibrium lies inside the hyperbox determined by α and z. If all equilibria are known, it is easy to check whether any one lies inside the hyperbox being constructed here. In fact, one can choose an appropriate unstable equilibrium to be the upper vertex.

In general, however, finding the upper vertex would require some search. A suitable search algorithm remains to be investigated. The computational cost of the proposed

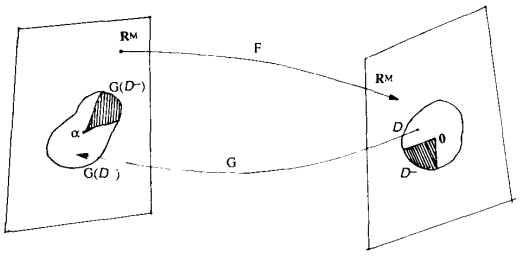

Fig. 5. The mappings F and G.

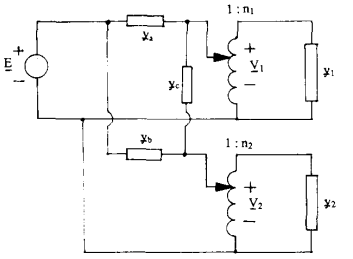

Fig. 6. Power system water study.

method is mainly the time to find vertices that satisfy the conditions of Lemma 6.

A sufficient condition for $\mathbf{N}_\alpha \neq \varnothing$ is that the Jacobian matrix at α is non-singular. If the condition is satisfied, then according to Lemma 6, α is asymptotically stable. The following proposition states the sufficient condition.

Proposition 4:

If the Jacobian matrix of the dynamical system (21) is *nonsingular at* α then the set $\mathbf{N}_\alpha$ as defined by (31) is nonempty. #

Proof: For convenience, define the following mapping:

$$F\colon \boldsymbol{x} \to (f_1(\boldsymbol{x}), \cdots, f_M(\boldsymbol{x}))$$

where $f_i(\cdot)$ is the RHS of (21), i.e., $dx_i/dt = f_i(\boldsymbol{x})$, $\forall i$. Note that α is a solution to $F(\boldsymbol{x}) = \mathbf{0}$, and the jacobian matrix of the dynamical system at α is $\partial F/\partial \boldsymbol{x}(\boldsymbol{x} = \alpha)$. If this matrix is non-singular then by the Inverse Function Theorem, F as a local inverse around $\mathbf{0}$, which is denoted, e.g., by G in Fig. 5. Let the domain of G be $\mathbf{D}$, and define $\mathbf{D}^- = \{\boldsymbol{d}\colon\ \boldsymbol{d} \in \mathbf{D},\ \boldsymbol{d} \leqslant \mathbf{0}\}$. Note that $G(\mathbf{D}^-) \subset \mathbf{N}_\alpha$. Thus $\mathbf{N}_\alpha \neq \varnothing$. ◆

Remark: It may seem that the condition given in Proposition 4 can be relaxed to isolation of α. However this may not be true. It has been found that for the 2-OLTC case, i.e., the power system used in Appendix 1, if there is only one equilibrium, it must be unstable [24]. This occurs when the curves $x_1 = L_1(x_2)$ and $x_2 = L_2(x_1)$ are tangent to each other. The Jacobian matrix is singular at this equilibrium, and $\mathbf{N}_\alpha = \varnothing$.

By investigating the Jacobian matrix explicitly, a much more simplified version of Proposition 4 can be obtained as follows:

Proposition 5:

If the matrix $\boldsymbol{X}(-\alpha_1^2, \cdots, -\alpha_M^2)$, where $\boldsymbol{X}(x_1^2, \cdots, x_M^2)$ is the matrix defined in (19), is nonsingular then the set $\mathbf{N}_\alpha$ is non-empty. #

Proof: It can be shown that the Jacobian matrix of (21) can be written in the following form:

$$\partial F/\partial \boldsymbol{x}(\text{at } \boldsymbol{x}) = \operatorname{diag}(1/T_1, \cdots, 1/T_M) \cdot \boldsymbol{Z}(\boldsymbol{x}) \cdot \operatorname{diag}(V_1(\boldsymbol{x}), \cdots, V_M(\boldsymbol{x}))$$

where $V_i(\boldsymbol{x})$ is the voltage at bus i due to the tap-settings $\boldsymbol{x} = (x_1, \cdots, x_M)$, and

$$\boldsymbol{Z}(\boldsymbol{x}) = 2 \cdot \operatorname{diag}(x_1, \cdots, x_M) \cdot \boldsymbol{X}^{-1} \cdot \operatorname{diag}(x_1, \cdots, x_M) - \boldsymbol{I}$$

Thus $\partial F/\partial \boldsymbol{x}$(at $\boldsymbol{x}$) is singular $\Leftrightarrow$ $\boldsymbol{Z}(\boldsymbol{x})$ is singular

$\Leftrightarrow 2 \cdot \operatorname{diag}(x_1, \cdots, x_M) \cdot \boldsymbol{X}^{-1} \cdot \operatorname{diag}(x_1, \cdots, x_M)$ has an eigenvalue 1

$\Leftrightarrow \operatorname{diag}(1/x_1, \cdots, 1/x_M) \cdot \boldsymbol{X} \cdot \operatorname{diag}(1/x_1, \cdots, 1/x_M)$ has an eigenvalue 2

$\Leftrightarrow 0 = \det\{\operatorname{diag}(1/x_1, \cdots, 1/x_M) \cdot \boldsymbol{X} \cdot \operatorname{diag}(1/x_1, \cdots, 1/x_M) - 2\boldsymbol{I}\}$

$\Leftrightarrow 0 = \det\{\boldsymbol{X} - 2 \cdot \operatorname{diag}(x_1^2, \cdots, x_M^2)\}$

$\Leftrightarrow \boldsymbol{X}(-x_1^2, \cdots, -x_M^2)$ is singular.

As a result, Proposition 5 follows directly from Proposition 4. ◆

V. An Illustration of Stability Region Constructed by Hyperboxes

To illustrate the construction of stability regions based on the proposed method, a simple power system of 2 interconnected OLTC's is shown in Fig. 6. Relative magnitudes of the power system parameters are also specified. In Fig. 7, each rectangular box with upper and lower corners in the regions $\mathbf{N}_\alpha$ and $\mathbf{P}_\alpha$, respectively, is an invariant set. Recall that a box with a corner in $\mathbf{N}_\alpha$ and a corresponding corner in $\mathbf{P}_\alpha$ is a stable hyperbox. The union of all such boxes is denoted by A, whose boundary is marked in the figure. The exact stability region [24] is also included for comparison with A. The stability region A is derived from Proposition 3. Note also that z_1, w_1 are the elements next to z, w, respectively, in the corresponding L-sequences. It has been shown that trajectories, starting from the w–z hyperbox, will enter the w_1–z_1 hyperbox in finite time.

VI. Conclusion

In this study, a mechanism of voltage collapse, namely, the OLTC action, is analyzed. A simple power system with one OLTC is analyzed first. System trajectories that lead to monotonic fall of bus voltages are constructed, which helps to explain the phenomena of voltage collapse. The analytical approach of the simple case is extended to the general M-bus power system model. For this model, it is

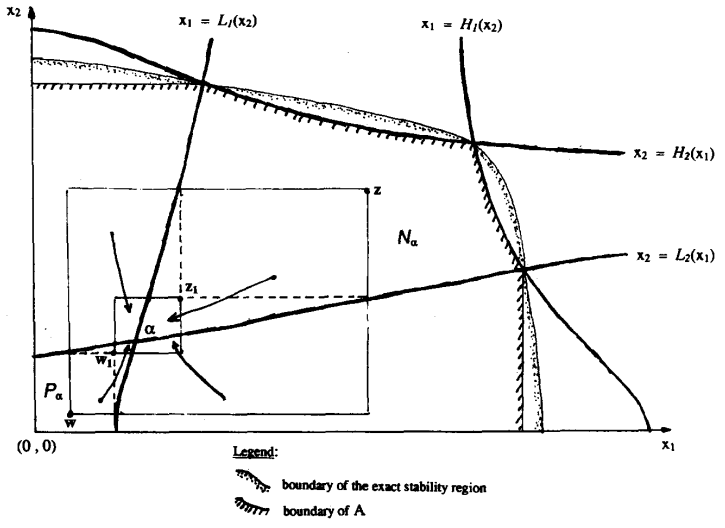

Fig. 7. Stability region for $M = 2$.

proved that there are as many as 2^M classes of equilibria, and only one class can contain a stable equilibrium. The issue of uniqueness of the stable equilibrium is still an open question.

A method is proposed which can be used to obtain a hyperbox subset of the true stability region. This paper identifies the smallest equilibrium from an invariant set and establishes the existence and stability of this equilibrium. The stability hyperboxes can be constructed around the smallest equilibrium. Since a single hyperbox may represent a small portion of the entire region, the union of hyperboxes can improve the result.

The instability of tap-changers is by no means the only mechanism that leads to voltage collapse. In reality many other factors are involved but not considered in our study. For example, the excitation system effects should be modelled in order to restrict the reactive power generation limits. Also, the impedance load model adopted in this study can be refined. A complex power demand with voltage dependency may be a good choice for the extension.

Appendix 1

Appendix 2

Let $A = (a_{ij})$ be an $n \times n$ (real) symmetric matrix with the following properties:

(a) irreducibly diagonally dominant [23];

(b) $a_{ii} > 0$ for $i = 1, \cdots, n$ and $a_{ij} \leqslant 0$ for $i, j = 1, \cdots, n$ and $j \neq i$;

and p be an $n \times 1$ (real) vector with $p_j \geqslant 0$ for $j = 1, \cdots, n$ where $p_j > 0$ for at least one j. Then

(i) the solution v to $Av = p$ is strictly positive;

(ii) $\Sigma_{j=1}^{n} A_{ij} p_j > 0$ for all $i = 1, \cdots, n$ where A_{ij} is the ij cofactor of A;

(iii) $A_{ij} > 0$ for all $i, j = 1, 2, \cdots, n$.

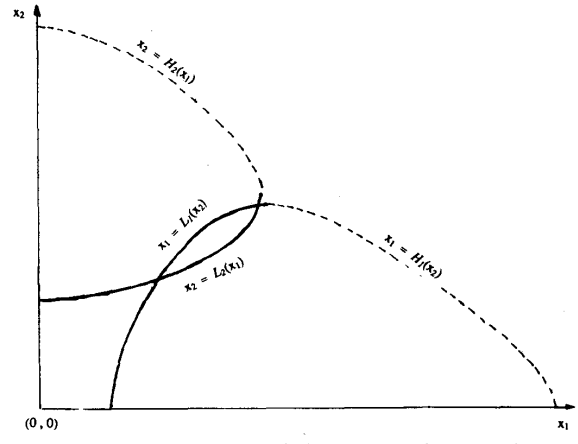

Fig. 8. A counterexample for which the class **L** has more than one equilibrium ($M = 2$, i.e., 2 tap-changers).

Proof: Omitted, see [24, pp. 47–48].

Appendix 3

Let A and p be as in Appendix 2, and v be the solution to $Av = p$. Let A^{ii} be the $(n-1) \times (n-1)$ matrix obtained by deleting row i and column i of A, and

$$w = (w_1, \cdots, w_{i-1}, w_{i+1}, \cdots, w_n)^T$$

be the solution to

$$A^{ii} w = (p_1, \cdots, p_{i-1}, p_{i+1}, \cdots, p_n)^T$$

then $w_k < v_k$ for $k = 1, \cdots, i-1, i+1, \cdots, n$.

Proof: Omitted, see [24, p. 49].

APPENDIX 4 (*Preparatory Fact for Lemma 1*)

(Refer to (19) for matrix X and its cofactors X_{ii}, X_{ij}'s.) The function

$$g_i(\cdot) = \frac{\left(\sum_{j=1}^{M+N} X_{ij}q_j\right)^2}{X_{ii}\left[b_{ii}X_{ii} + \sum_{j=1,\, j\neq i}^{M+N} - b_{ij}X_{ij}\right]}$$

of $M-1$ variables $(x_1,\cdots,x_{i-1},x_{i+1},\cdots,x_M)$ is strictly decreasing and its infimum is q_i^2/b_{ii}.

Proof: It shall be shown that $\partial g_i/\partial x_k < 0$ when $x_k > 0$ for $i,\ k=1,\cdots,M$ and $k\neq i$. Without loss of generality one can assume $i=1$ and $k=2$. It is sufficient to consider the numerator of $\partial g_1/\partial x_2$ (since the denominator is always >0). One has

$$\begin{aligned}\text{Num}\{\partial g_1/\partial x_2\} &= \left(\sum_j X_{1j}q_j\right)\Bigg\{2\partial/\partial x_2\left(\sum_j X_{1j}q_j\right)\\ &\cdot X_{11}\left(b_{11}X_{11} + \sum_{j\neq 1} - b_{1j}X_{1j}\right)\\ &-\left(\sum_j X_{1j}q_j\right)\partial X_{11}/\partial x_2\left(b_{11}X_{11} + \sum_{j\neq 1} - b_{1j}X_{1j}\right)\\ &-\left(\sum_j X_{1j}q_j\right)X_{11}\partial/\partial x_2\left(b_{11}X_{11} + \sum_{j\neq 1} - b_{1j}X_{1j}\right)\Bigg\}.\end{aligned}$$

As a result of Appendix 2, $\sum_j X_{1j}q_j > 0$. So if one can show that

(a)

$$\partial/\partial x_2\left(\sum_j X_{1j}q_j\right)X_{11}\left(b_{11}X_{11} + \sum_{j\neq 1} - b_{1j}X_{1j}\right) \leqslant \left(\sum_j X_{1j}q_j\right)\partial X_{11}/\partial x_2\left(b_{11}X_{11} + \sum_{j\neq 1} - b_{1j}X_{1j}\right)$$

and that

(b)

$$\partial/\partial x_2\left(\sum_j X_{1j}q_j\right)X_{11}\left(b_{11}X_{11} + \sum_{j\neq 1} - b_{1j}X_{1j}\right) < \left(\sum_j X_{1j}q_j\right)X_{11}\partial/\partial x_2\left(b_{11}X_{11} + \sum_{j\neq 1} - b_{1j}X_{1j}\right)$$

for $x_2 > 0$ then it implies that $\text{Num}\{\partial g_1/\partial x_2\} < 0$ when $x_2 > 0$.

In (a) and (b), it can be shown that each side of the inequalities is a product of 3 positive terms; therefore, (a) and (b) are equivalent to

(a1)
$$\frac{\partial/\partial x_2\left(\sum_j X_{1j}q_j\right)}{\partial X_{11}/\partial x_2} \leqslant \frac{\sum_j X_{1j}q_j}{X_{11}}$$

and

(b1)
$$\frac{\partial/\partial x_2\left(\sum_j X_{1j}q_j\right)}{\partial/\partial x_2\left(b_{11}X_{11} + \sum_{j\neq 1} - b_{1j}X_{1j}\right)} < \frac{\sum_j X_{1j}q_j}{\left(b_{11}X_{11} + \sum_{j\neq 1} - b_{1j}X_{1j}\right)}$$

respectively.

Now define

(1) $\boldsymbol{A}$ be the matrix obtained by replacing column 1 of $\boldsymbol{X}$ by $(q_1,\cdots,q_M,\cdots,q_{M+N})^T$.

(2) $\boldsymbol{B}$ be the matrix obtained by replacing column 1 of $\boldsymbol{X}$ by $(1,0,\cdots,0)^T$.

(3) $\boldsymbol{C}$ be the matrix obtained by replacing column 1 of $\boldsymbol{X}$ by $(b_{11},-b_{21},\cdots,-b_{M+N,1})^T$.

and $\boldsymbol{A}^{22},\boldsymbol{B}^{22},\boldsymbol{C}^{22}$ be the matrices obtained from $\boldsymbol{A},\boldsymbol{B},\boldsymbol{C}$ be deleting row 2 and column 2. That is, for instance,

$$\boldsymbol{A} = \left[\begin{array}{ccccc|ccc} q_1 & -b_{12} & \cdots & & -b_{1M} & -b_{1,M+1} & \cdots & -b_{1,M+N} \\ q_2 & x_2^2+b_{22} & \cdots & & -b_{2M} & -b_{2,M+1} & \cdots & -b_{2,M+N} \\ q_3 & -b_{32} & x_3^2+b_{33} & \cdots & -b_{3M} & -b_{3,M+1} & \cdots & -b_{3,M+N} \\ \vdots & \vdots & \vdots & & \vdots & \vdots & & \vdots \\ q_M & -b_{M2} & -b_{M3} & & x_M^2+b_{MM} & -b_{M,M+1} & \cdots & -b_{M,M+N} \\ \hline q_{M+1} & -b_{M+1,2} & -b_{M+1,3} & \cdots & -b_{M+1,M} & b_{M+1,M+1} & \cdots & -b_{M+1,M+N} \\ q_{M+N} & -b_{M+N,2} & -b_{M+N,3} & & \cdot & \cdot & & b_{M+N,M+N} \end{array}\right]$$

and so on. Then (a1) and (b1) are, respectively, equivalent to

(a2) $\det(\boldsymbol{A}^{22})/\det(\boldsymbol{B}^{22}) \leqslant \det(\boldsymbol{A})/\det(\boldsymbol{B})$

(b2) $\det(\boldsymbol{A}^{22})/\det(\boldsymbol{C}^{22}) < \det(\boldsymbol{A})/\det(\boldsymbol{C})$

Using Cramer's rule one obtains the following.

(1) The left-hand side of (a2) is the first component w_1 of $\boldsymbol{w}=(w_1,w_3,\cdots,w_{M+N})^T$ in $\boldsymbol{B}^{22}\boldsymbol{w}=(q_1,q_3,\cdots,q_{M+N})^T$ and its right-hand side is the first component v_1 of $\boldsymbol{v}=(v_1,v_2,\cdots,v_{M+N})^T$ in $\boldsymbol{B}\boldsymbol{v}=(q_1,q_2,q_3,\cdots,q_{M+N})^T$. It shall be proved that $w_1 \leqslant v_1$. Note that $(v_2,v_3,\cdots,v_{M+N})^T$ is the solution to

$$\boldsymbol{B}^{11}(v_2,v_3,\cdots,v_{M+N})^T = (q_2,q_3,\cdots,q_{M+N})^T$$

and that $(w_3,\cdots,w_{M+N})^T$ is the solution to

$$[\boldsymbol{B}^{11}]^{11}(w_3,\cdots,w_{M+N})^T = (q_3,\cdots,q_{M+N})^T$$

where $\boldsymbol{B}^{11}$ is the matrix obtained by deleting row 1 and

column 1 of $\boldsymbol{B}$, and $[\boldsymbol{B}^{11}]^{11}$ by deleting row 1 and column 1 of $\boldsymbol{B}^{11}$.

If $q_2 = q_3 = \cdots = q_{M+N} = 0$ then $v_2 = v_3 = \cdots = v_{M+N} = 0$ and $w_3 = w_4 = \cdots = w_{M+N} = 0$; thus $w_1 = v_1 = q_1$. And if $q_j \neq 0$ for some $j \geq 2$ then from Appendix 2, one has $v_2 > 0, v_3 > w_3 \geq 0, \cdots, v_{M+N} > w_{M+N} \geq 0$. Multiplying the first row of $\boldsymbol{B}$ by $\boldsymbol{v}$ and the first row of $\boldsymbol{B}^{22}$ by $\boldsymbol{w}$, one obtains

$$v_1 - b_{12}v_2 - \sum_{k=3} b_{1k}v_k = q_1$$

and

$$w_1 - \sum_{k=3} b_{1k}w_k = q_1$$

respectively.

Subtracting w_1 from v_1 and rearranging terms, one gets

$$v_1 - w_1 = b_{12}v_2 + \sum_{k=3} b_{1k}(v_k - w_k)$$

which is positive since at least one of the b-coefficients is positive and $v_2 > 0$, $v_3 > w_3, \cdots, v_{M+N} > w_{M+N}$. Thus (a2) is proved.

(2) The left-hand side of (b2) is the first component w_1 of $\boldsymbol{w} = (w_1, w_3, \cdots, w_{M+N})^T$ in $\boldsymbol{C}^{22}\boldsymbol{w} = (q_1, q_3, \cdots, q_{M+N})^T$ and its right-hand side is the first component v_1 of $\boldsymbol{v} = (v_1, v_2, \cdots, v_{M+N})^T$ in $\boldsymbol{Cv} = (q_1, q_2, q_3, \cdots, q_{M+N})^T$. A direct application of Appendix 3 gives $v_1 > w_1$. Thus (b2) is true.

Therefore one can conclude that $\{\partial g_1/\partial x_2\} < 0$, for $x_2 > 0$. Similarly, $\partial g_1/\partial x_3 < 0$, etc. Since it is bounded below (by 0, for instance) g_1 has infimum. The infimum is the value of g_1 at $(\infty, \infty, \cdots, \infty)$. The function $g_1(\cdot)$ has the structure of a rational polynomial. Thus its value at $(\infty, \infty, \cdots, \infty)$ is the ratio of the two coefficients associated with the terms of highest order in the numerator and the denominator; the result is q_1^2/b_{11}. ◆

Appendix 5 (*Proof of Lemma 2*)

For each $i = 1, 2, \cdots, M$ and $j = 1, \cdots, i-1, i+1, \cdots, M$, $\partial L_i/\partial x_j > 0$ and $\partial H_i/\partial x_j < 0$ when $x_j > 0$ and $\partial L_i/\partial x_j = \partial H_i/\partial x_j = 0$ when $x_j = 0$.

Proof: Only the case $i = 1$, $j = 2$ is considered here. Recall that the two functions $x_1 = L_1(x_2, \cdots, x_M)$ and $x_1 = H_1(x_2, \cdots, x_M)$ satisfy (23), i.e.,

$$0 = x_1^2[\sqrt{\bar{y}_1}V_{1o}X_{11}] - x_1\left[\sum_{k=1}^{M+N} X_{1k}q_k\right] + \sqrt{\bar{y}_1}V_{1o}\left(b_{11}X_{11} + \sum_{k=1,\,k\neq 1}^{M+N} - b_{1k}X_{1k}\right). \quad \text{(A.5-1)}$$

$\partial x_1/\partial x_2$ can be derived from (A.5-1) as

$$\frac{\partial x_1}{\partial x_2} = \frac{x_1^2[\sqrt{\bar{y}_1}V_{1o}\partial X_{11}/\partial x_2] - x_1\sum_k \partial X_{1k}/\partial x_2 q_k + \sqrt{\bar{y}_1}V_{1o}\left[b_{11}\partial X_{11}/\partial x_2 + \sum_{k\neq 1} - b_{1k}\partial X_{1k}/\partial x_2\right]}{-2x_1\sqrt{\bar{y}_1}V_{1o}X_{11} + \sum_k X_{1k}q_k}. \quad \text{(A.5-2)}$$

Consider the numerator and the denominator of (A.5-2) separately. Using (A.5-1) to eliminate the term x_1^2, and after some simple manipulations, one can rewrite the numerator of (A.5-2) as

$$\text{num} = 1/X_{11}\left[\partial X_{11}/\partial x_2 \sum_{k\neq 1}(x_1q_k + \sqrt{\bar{y}_1}V_{1o}b_{1k})X_{1k} - X_{11}\partial/\partial x_2\left(\sum_{k\neq 1}(x_1q_k + \sqrt{\bar{y}_1}V_{1o}b_{1k})X_{1k}\right)\right]. \quad \text{(A.5-3)}$$

When $x_2 = 0$, (A.5-3) is equal to 0 since each $\partial X_{1k}/\partial x_2$ $(k = 1, \cdots, M)$ contains $2x_2$ as a factor. When $x_2 > 0$, it is to be proved that the numerator (A.5-3) is > 0, which is equivalent to (since each term is > 0)

$$\frac{\partial/\partial x_2 \sum_{k\neq 1}(x_1q_k + \sqrt{\bar{y}_1}V_{1o}b_{1k})X_{1k}}{\partial/\partial x_2 X_{11}} < \frac{\sum_{k\neq 1}(x_1q_k + \sqrt{\bar{y}_1}V_{1o}b_{1k})X_{1k}}{X_{11}}. \quad \text{(A.5-4)}$$

Let

(1) $\boldsymbol{A}$ be the matrix obtained by replacing column 1 of $\boldsymbol{X}$ by

$$(x_1q_1 + \sqrt{\bar{y}_1}V_{1o}b_{11}, \cdots, x_1q_{M+N} + \sqrt{\bar{y}_1}V_{1o}b_{1,M+N})^T.$$

(2) $\boldsymbol{B}$ be the matrix obtained by replacing column 1 of $\boldsymbol{X}$ by $(1, 0, \cdots, 0)^T$.

Then (A.5-4) becomes

$$\det(\boldsymbol{A}^{22})/\det(\boldsymbol{B}^{22}) < \det(\boldsymbol{A})/\det(\boldsymbol{B}) \quad \text{(A.5-5)}$$

where $\boldsymbol{A}^{22}$ and $\boldsymbol{B}^{22}$ are matrices obtained by deleting row 2 and column 2 of $\boldsymbol{A}$ and $\boldsymbol{B}$, respectively. Following a similar technique as in Appendix 4, it is seen that (A.5-5) is indeed true. Thus the numerator of (A.5-2) is always > 0.

Next the denominator of (A.5-2) is considered. It shall be shown that the denominator is < 0 for $x_1 = H_1(\cdot)$ and is > 0 for $x_1 = L_1(\cdot)$, which is equivalent to

$$L_1(\cdot) < \frac{\sum_k X_{1k}q_k}{2\sqrt{\bar{y}_1}V_{1o}X_{11}} < H_1(\cdot) \text{ whenever } L_i(\cdot) \neq H_i(\cdot). \quad \text{(A.5-6)}$$

Equation (A.5-6) is true since 1) $x_1 = \sum_k X_{1k}q_k/2\sqrt{\bar{y}_1}V_{1o}X_{11}$ makes the RHS of (A.5-1) negative, and 2) since the leading coefficient of the RHS is positive. Thus $\sum_k X_{1k}q_k/2\sqrt{\bar{y}_1}V_{1o}X_{11}$ lies between the roots $L_1(\cdot)$ and

$H_1(\cdot)$ of (A.5-1) whenever these two roots are distinct. Further note that if $L_1(\cdot) = H_1(\cdot)$ then (A.5-6) becomes an equality, and that $\partial H_1/\partial x_2 = -\infty$, $\partial L_1/\partial x_2 = +\infty$. ◆

APPENDIX 6 (*Proof of Lemma 3*)

It shall be shown that a trajectory starting at a point inside $\boldsymbol{P}$ or $\boldsymbol{N}$ does not leave the region. It is sufficient to consider a boundary point as the starting point.

Let z be an arbitrary point on the boundary of $\boldsymbol{P}$ or $\boldsymbol{N}$, then $dx_i(z)/dt = 0$ for some i. Suppose that $dx_i(z)/dt \neq 0$ for some $j \neq i$ (otherwise z is an equilibrium and the trajectory is trivial). Without loss of generality assume that $i = 1$, i.e., $dx_1(z)/dt = 0$. The term $d^2x_1(z)/dt^2$ will be investigated.

Differentiating (21), one obtains

$$\frac{d^2x_1}{dt^2} = \frac{1}{T_1}\left(-\frac{dx_1}{dt}\cdot\frac{\sum_{j=1}^{M+N} X_{1j}q_j}{\det(\boldsymbol{X})} - x_1\cdot\sum_{k=1}^{M}\frac{\partial}{\partial x_k}\left[\frac{\sum_{j=1}^{M+N} X_{1j}q_j}{\det(\boldsymbol{X})}\right]\cdot\frac{dx_k}{dt}\right). \quad \text{(A.6-1)}$$

Evaluating (A.6-1) at z, since $dx_1(z)/dt = 0$ by assumption,

$$\frac{d^2x_1}{dt^2}(z) = \frac{1}{T_1}\left(- z_1\cdot\sum_{k=2}^{M}\frac{\partial}{\partial x_k}\left[\frac{\sum_{j=1}^{M+N} X_{1j}q_j}{\det(\boldsymbol{X})}\right]\cdot\frac{dx_k}{dt}(z)\right). \quad \text{(A.6-2)}$$

One can always assume that $z > \mathbf{0}$, for if $z_i = 0$, $dx_i/dt(\boldsymbol{x} = z) > 0$ by (21). The following inequality will be established:

$$\frac{\partial}{\partial x_k}\sum_{j=1}^{M+N}\frac{X_{1j}q_j}{\det(\boldsymbol{X})} < 0, \qquad \text{for each } k = 2,3,\cdots,M. \quad \text{(A.6-3)}$$

Only the case of $k = 2$ will be given here; others are similar. Equation (A.6-3) is, for $k = 2$, equivalent to

$$\frac{\partial/\partial x_2\sum_j X_{1j}q_j}{\partial/\partial x_2\det(\boldsymbol{X})} < \frac{\sum_j X_{1j}q_j}{\det(\boldsymbol{X})} \quad \text{(A.6-4)}$$

The RHS of (A.6-4) is the first component v_1 of $\boldsymbol{v} = (v_1, v_2, \cdots, v_M)^T$ in $\boldsymbol{X}\cdot\boldsymbol{v} = (q_1, q_2, \cdots, q_{M+N})^T$. The LHS of (A.6-4) is the first component w_1 of $\boldsymbol{w} = (w_1, w_3, \cdots, w_{M+N})^T$ in $\boldsymbol{X}^{22}\cdot\boldsymbol{w} = (q_1, q_3, \cdots, q_{M+N})^T$, where $\boldsymbol{X}^{22}$ denotes the submatrix of $\boldsymbol{X}$ obtained by deleting row 2 and column 2. Thus, (A.6-4) is true by Appendix 3. As a result, (A.6-3) is established and (A.6-2) takes the form

$$d^2x_1(z)/dt^2 = \sum_{k\neq 1} a_{k,1}dx_k(z)/dt \text{ where } a_{k,1} > 0 \text{ for all } k.$$

In summary,

$$\frac{dx_i}{dt}(z) = 0 \Rightarrow \frac{d^2x_i}{dt^2}(z) = \sum_{k=1,\,k\neq i}^{M} a_{k,i}\frac{dx_k}{dt}(z) \text{ where } a_{k,i} > 0. \quad \text{(A.6-5)}$$

Now if $z \in \mathbf{P}$ (and z is not an equilibrium) then $dx_k(z)/dt \geqslant 0$ by definition and the strict inequality holds for at least one k. Referring to (A.6-5) one sees that for those i with $dx_i(z)/dt = 0$, $d^2x_i(z)/dt^2 > 0$, which means that dx_i/dt stays positive during some time interval after the trajectory leaves z. Also, for those i with $dx_i(z)/dt > 0$, dx_i/dt remains positive during some time interval after the trajectory leaves z since dx_i/dt is continuous. Thus dx_i/dt stays positive for all i during a time interval after the trajectory leaves z. This proves that $\mathbf{P}$ is an invariant set.

If $z \in \mathbf{N}$, similar arguments can be used to obtain that $\mathbf{N}$ is an invariant set. ◆

APPENDIX 7 (*Proof of Proposition 1*)

Let $\boldsymbol{b}$ be an equilibrium for which

$$b_i = H_i(b_1,\cdots,b_{i-1},b_{i+1},\cdots,b_M) > L_i(b_1,\cdots,b_{i-1},b_{i+1},\cdots,b_M) \text{ for some } i.$$

First it will be shown that $\mathbf{N}$ contains points arbitrarily close to $\boldsymbol{b}$. Choose an arbitrary number ϵ with $0 < \epsilon < H_i(b_1,\cdots,b_{i-1},b_{i+1},\cdots,b_M) - L_i(b_1,\cdots,b_{i-1},b_{i+1},\cdots,b_M)$. Define $\boldsymbol{a}$ as follows

$$a_k = b_k, \qquad \text{for } k \neq i$$
$$a_i = b_i - \epsilon. \quad \text{(A.7-1)}$$

Then

$$L_i(a_1,\cdots,a_{i-1},a_{i+1},\cdots,a_M) = L_i(b_1,\cdots,b_{i-1},b_{i+1},\cdots,b_M) < H_i(b_1,\cdots,b_{i-1},b_{i+1},\cdots,b_M) - \epsilon = b_i - \epsilon = a_i$$

and

$$a_i < b_i = H_i(b_1,\cdots,b_{i-1},b_{i+1},\cdots,b_M) = H_i(a_1,\cdots,a_{i-1},a_{i+1},\cdots,a_M)$$

which indicates that $dx_i(\boldsymbol{a})/dt < 0$ (Property 1(b)). Also, for $k \neq i$,

$$L_k(a_1,\cdots,a_{k-1},a_{k+1},\cdots,a_M) < L_k(b_1,\cdots,b_{k-1},b_{k+1},\cdots,b_M) \leqslant b_k \leqslant H_k(b_1,\cdots,b_{k-1},b_{k+1},\cdots,b_M) < H_k(a_1,\cdots,a_{k-1},a_{k+1},\cdots,a_M)$$

where the strict inequalities are due to monotonicity of H_k and L_k, and the second and third inequalities follows from the fact that $\boldsymbol{b}$ is an equilibrium. Thus, $dx_k(\boldsymbol{a})/dt < 0$ for

all k (Property 1). In other words, it is found that **N** contains an interior point $\boldsymbol{a}$ arbitrarily close to the equilibrium $\boldsymbol{b}$.

Take any such $\boldsymbol{a}$ and consider the trajectory passing through $\boldsymbol{a}$. Since **N** is invariant, bounded and $dx_k/dt \leqslant 0$ in **N**, the trajectory must be convergent. It is easy to see that the limit point is an equilibrium, which is different from $\boldsymbol{b}$. If there are finitely many equilibria, instability of $\boldsymbol{b}$ is immediately obtained. In case that a continuum of equilibria exists, further work is needed as shown below.

Let $\boldsymbol{e}$ be any equilibrium that is not in **L**, that is, $e_k = H_k(e_1, \cdots, e_{k-1}, e_{k+1}, \cdots, e_M)$ for some k. Assume that the above-mentioned trajectory were to converge to $\boldsymbol{e}$, then it must be true that $\boldsymbol{a} \geqslant \boldsymbol{e}$, with inequality holds for at least one j, i.e., $a_j > e_j$. Consider the kth components,

$$\begin{aligned} &H_k(a_1, \cdots, a_{k-1}, a_{k+1}, \cdots, a_M) \\ &\quad \geqslant a_k \geqslant e_k \\ &\quad = H_k(e_1, \cdots, e_{k-1}, e_{k+1}, \cdots, e_M) \end{aligned} \quad \text{(A.7-2)}$$

where the first inequality is due to the fact that dx_k/dt(at $\boldsymbol{a}$) $\leqslant 0$ (Property 1). Since H_k is a decreasing function,

$$\begin{aligned} &H_k(a_1, \cdots, a_{k-1}, a_{k+1}, \cdots, a_M) \\ &\quad \leqslant H_k(e_1, \cdots, e_{k-1}, e_{k+1}, \cdots, e_M). \end{aligned} \quad \text{(A.7-3)}$$

Thus (A.7-2) and (A.7-3) imply that

$$\begin{aligned} &H_k(a_1, \cdots, a_{k-1}, a_{k+1}, \cdots, a_M) \\ &\quad = a_k = e_k \\ &\quad = H_k(e_1, \cdots, e_{k-1}, e_{k+1}, \cdots, e_M). \end{aligned} \quad \text{(A.7-4)}$$

However, this contradicts the fact that $\boldsymbol{a} \geqslant \boldsymbol{e}$ (with $a_j > e_j$) and H_k is strictly decreasing. In other words, the trajectory must converge to a point in **L**. The instability of $\boldsymbol{b}$ follows since the class **L** is isolated from the other classes.

Appendix 8 (*Proof of Lemma 4*)

Only the work for Case (2) is shown; that for Case (1) is similar but simpler. First it is shown inductively that the L-sequence starting at $\boldsymbol{x}$ contains an infinite number of elements.

Assume that $\boldsymbol{a}_k$ satisfies the following conditions:

i) $z_i \leqslant L_i(z_1, \cdots, z_{i-1}, z_{i+1}, \cdots, z_M)$, $i = 1, \cdots, M$ (with at least one strict inequality).

ii) $\boldsymbol{z} \leqslant \boldsymbol{b}$.

It shall be shown that $\boldsymbol{a}_{k+1}$ is well defined, $\boldsymbol{a}_{k+1} \geqslant \boldsymbol{a}_k (\boldsymbol{a}_{k+1} \neq \boldsymbol{a}_k)$, and $\boldsymbol{a}_{k+1}$ satisfies both i) and ii). Since for each i, $L_i((\boldsymbol{a}_k)_1, \cdots, (\boldsymbol{a}_k)_{i-1}, (\boldsymbol{a}_k)_{i+1}, \cdots, (\boldsymbol{a}_k)_M)$ exists by induction assumption, $\boldsymbol{a}_{k+1}$ is well defined. Let j be a component for which strict inequality in i) holds for $\boldsymbol{a}_k$, i.e.,

$$(\boldsymbol{a}_k)_j < L_j((\boldsymbol{a}_k)_1, \cdots, (\boldsymbol{a}_k)_{j-1}, (\boldsymbol{a}_k)_{j+1}, \cdots, (\boldsymbol{a}_k)_M). \quad \text{(A.8-1)}$$

For each component $i \neq j$,

$$\begin{aligned} (\boldsymbol{a}_{k+1})_i &= L_i((\boldsymbol{a}_k)_1, \cdots, (\boldsymbol{a}_k)_{i-1}, (\boldsymbol{a}_k)_{i+1}, \cdots, (\boldsymbol{a}_k)_M) \\ &\geqslant (\boldsymbol{a}_k)_i, \text{ from condition i), and} \\ b_i &= L_i(b_1, \cdots, b_{i-1}, b_{i+1}, \cdots, b_M) \\ &\geqslant L_i((\boldsymbol{a}_k)_1, \cdots, (\boldsymbol{a}_k)_{i-1}, (\boldsymbol{a}_k)_{i+1}, \cdots, (\boldsymbol{a}_k)_M) \\ &= (\boldsymbol{a}_{k+1})_i. \end{aligned}$$

For component j, similar inequalities yield $(\boldsymbol{a}_{k+1})_j > (\boldsymbol{a}_k)_j$ (note strict inequality), and $b_j \geqslant (\boldsymbol{a}_k)_j$. Thus $\boldsymbol{a}_k \leqslant \boldsymbol{a}_{k+1} \leqslant \boldsymbol{b}$ and $\boldsymbol{a}_k \neq \boldsymbol{a}_{k+1}$. Since each L_n is defined at $(b_1, \cdots, b_{n-1}, b_{n+1}, \cdots, b_M)$, it must be defined at $((\boldsymbol{a}_{k+1})_1, \cdots, (\boldsymbol{a}_{k+1})_{n-1}, (\boldsymbol{a}_{k+1})_{n+1}, \cdots, (\boldsymbol{a}_{k+1})_M)$ by (3) of Lemma 1. Using $\boldsymbol{a}_k \leqslant \boldsymbol{a}_{k+1}$ together with (A.8-1), one can write

$$\begin{aligned} (\boldsymbol{a}_{k+1})_i &= L_i((\boldsymbol{a}_k)_1, \cdots, (\boldsymbol{a}_k)_{i-1}, (\boldsymbol{a}_k)_{i+1}, \cdots, (\boldsymbol{a}_k)_M) \\ &< L_i((\boldsymbol{a}_{k+1})_1, \cdots, (\boldsymbol{a}_{k+1})_{i-1}, \\ &\quad (\boldsymbol{a}_{k+1})_{i+1}, \cdots, (\boldsymbol{a}_{k+1})_M), \qquad \text{for } i \neq j. \end{aligned} \quad \text{(A.8-2)}$$

For component j, the above strict inequality is replaced by weak inequality, i.e.,

$$\begin{aligned} (\boldsymbol{a}_{k+1})_j &= L_j((\boldsymbol{a}_k)_1, \cdots, (\boldsymbol{a}_k)_{j-1}, (\boldsymbol{a}_k)_{j+1}, \cdots, (\boldsymbol{a}_k)_M) \\ &\leqslant L_j((\boldsymbol{a}_{k+1})_1, \cdots, (\boldsymbol{a}_{k+1})_{j-1}, \\ &\quad (\boldsymbol{a}_{k+1})_{j+1}, \cdots, (\boldsymbol{a}_{k+1})_M). \end{aligned} \quad \text{(A.8-3)}$$

In other words, it has been proven that if i) and ii) hold for $\boldsymbol{a}_k$ they also hold for $\boldsymbol{a}_{k+1}$. Thus the sequence $\{\boldsymbol{a}_k\}$ has infinitely many elements, and is decreasing in such a way that $\boldsymbol{a}_k \leq \boldsymbol{a}_{k+1}$ and $\boldsymbol{a}_k < \boldsymbol{a}k + 2$, $\forall k$.

Since this (increasing) sequence is bounded above by $\boldsymbol{b}$, it converges to some $\boldsymbol{a} \leqslant \boldsymbol{b}$ (note that $\boldsymbol{a}_0 < \boldsymbol{a}$, with strict inequality). The fact that L_i's are continuous implies that $\boldsymbol{a} \in \mathbf{L}$. ◆

Appendix 9 (*Proof of Lemma 5*)

First it should be pointed out that $\mathbf{P}_\alpha$ is nontrivial, i.e., it does not contain α alone. Since $dx/dt(\mathbf{0}) > \mathbf{0}$, $\mathbf{0} \in \mathbf{P}_\alpha$.

Next, it shall be shown that:

$$\begin{aligned} &\boldsymbol{b} \text{ is on the boundary of } \{\boldsymbol{x}: \mathbf{0} \leqslant \boldsymbol{x} \leqslant \alpha\} \\ &\qquad \text{and } \boldsymbol{b} \neq \alpha \Rightarrow \boldsymbol{b} \notin \{\boldsymbol{x}: d\boldsymbol{x}/dt \geqslant \mathbf{0}\}. \end{aligned} \quad \text{(A.9-1)}$$

Take any $\boldsymbol{b}$ on the boundary of $\{\boldsymbol{x}: \leqslant \boldsymbol{x} \leqslant \alpha\}$ and $\boldsymbol{b} \neq \alpha$. Then $\boldsymbol{b} \leqslant \alpha$ with $b_j < \alpha_j$ and $b_k = \alpha_k$ for some components j and k. As a result,

$$\begin{aligned} &L_k(b_1, \cdots, b_{k-1}, b_{k+1}, \cdots, b_M) \\ &\quad < L_k(\alpha_1, \cdots, \alpha_{k-1}, \alpha_{k+1}, \cdots, \alpha_M) = \alpha_k = b_k \\ &\quad \text{and } b_k = \alpha_k \leqslant H_k(\alpha_1, \cdots, \alpha_{k-1}, \alpha_{k+1}, \cdots, \alpha_M) \\ &\quad < H_k(b_1, \cdots, b_{k-1}, b_{k+1}, \cdots, b_M) \end{aligned}$$

which indicates that $dx_k/dt(\boldsymbol{x} = \boldsymbol{b}) < 0$. Thus (A.9-1) is true.

Finally, let $\boldsymbol{p} \in \mathbf{P}_\alpha$, $\boldsymbol{p} \neq \alpha$, be given, and consider the trajectory passing through $\boldsymbol{p}$. Lemma 3 states that this trajectory will stay within the set $\{\boldsymbol{x}: d\boldsymbol{x}/dt \geqslant \mathbf{0}\}$ for all future times. Thus by (A.9-1), the trajectory cannot reach

the boundary of $\{x: \leqslant x \leqslant \alpha\}$. In other words, not only the trajectory stays in $\{x: dx/dt \geqslant \mathbf{0}\}$, it also stays within $\{x: \leqslant x \leqslant \alpha\}$. This proves that $\mathbf{P}_\alpha$ is invariant. It is now clear that the trajectory must converge to an equilibrium e, with $e \leqslant \alpha$ (for $x(t)$ is bounded above by α). Since α is the smallest equilibrium, $e = \alpha$. ◆

APPENDIX 10: (*Proof of Lemma 6*)

First, it is shown that

$\forall w \in \mathbf{P}_\alpha, \forall z \in \mathbf{N}_\alpha,$

the hyperbox $\{x: w \leqslant x \leqslant z\}$ is invariant. (A.10-1)

Given any $w \in \mathbf{P}_\alpha$, $z \in \mathbf{N}_\alpha$, the set $\{x: w \leqslant x \leqslant z\}$ is non-empty since $w \leqslant \alpha < z$ (Proposition 2). Take any b within this set. Consider the trajectory $x(t)$, $t \geqslant 0$, with $x(0) = b$. It shall be shown that $x(t)$ stays within the hyperbox for some non-empty time interval $[0, t_0)$. One can always assume that $b \neq w$ and $b \neq z$ (for if $b = w$ or $b = z$, the trajectory converges monotonically to α). Consider each component, one has:

i) For those i with $b_i = w_i$,

$$b_i = w_i \leqslant L_i(w_1, \cdots, w_{i-1}, w_{i+1}, \cdots, w_M) < L_i(b_1, \cdots, b_{i-1}, b_{i+1}, \cdots, b_M)$$

where the strict inequality is due to the fact that $w \leqslant b$, $w \neq b$ and L_i is strictly increasing. Thus $dx_i/dt(x = b) > 0$, and since $w_i = b_i < z_i$, it implies that $w_i \leqslant x_i(t) \leqslant z_i$ during a non-empty time interval $[0, t_i)$.

ii) Similarly, for those j with $b_j = z_j$,

$$\begin{aligned} L_j(b_1, \cdots, b_{j-1}, b_{j+1}, \cdots, b_M) &< L_j(z_1, \cdots, z_{j-1}, z_{j+1}, \cdots, z_M) \leqslant z_j = b_j \\ &= z_j \leqslant H_j(z_1, \cdots, z_{j-1}, z_{j+1}, \cdots, z_M) \\ &< H_j(b_1, \cdots, b_{j-1}, b_{j+1}, \cdots, b_M) \end{aligned}$$

which indicates that $dx_j/dt(x = b) < 0$. Since $w_j < b_j = z_j$, it implies that $w_j \leqslant x_j(t) \leqslant z_j$ during a non-empty time interval $[0, t_j)$.

iii) For those k with $w_k < b_k < z_k$, $w_k \leqslant x_k(t) \leqslant z_k$ during some nonempty $[0, t_k)$.

Combining the above possibilities, it is seen that the trajectory stays within the hyperbox during a nonempty time interval after leaving b. Since b is chosen arbitrarily, it implies that the hyperbox is invariant. In other words, (A.10-1) is true.

Next the following is to be shown:

the hyperbox $\{x: w \leqslant x \leqslant z\}$ is a region of attraction,

$$\forall w \in \mathbf{P}_\alpha, \forall z \in \mathbf{N}_\alpha. \quad \text{(A.10-2)}$$

Given $w \in \mathbf{P}_\alpha$ and $z \in \mathbf{N}_\alpha$ denote the L-sequences starting at w and z by $\{w_k, k = 0, 1, \cdots\}$ and $\{z_k, k = 0, 1, \cdots\}$, respectively. It is easily seen that these sequences are confined to $\mathbf{P}_\alpha$ and $\mathbf{N}_\alpha$ respectively, and they both converge monotonically to α (more precisely, w_k converges increasingly and z_k converges decreasingly). For each k, $k = 0, 1, \cdots$, the points w_k and z_k define a hyperbox, which is denoted by $B(w_k, z_k)$. Since the sequences of points w_k and z_k converge monotonically to α, one has (1) $B(w_k, z_k) \supset B(w_{k+1}, z_{k+1}) \forall k$, and (2) $B(w_k, z_k)$ shrinks to α as $k \to \infty$. Therefore, by showing that the trajectory enters the hyperbox $B(w_{k+1}, z_{k+1})$ from $B(w_k, z_k)$, $\forall k = 0, 1, \cdots$, the asymptotical stability of α results. Strictly speaking, the proof must be done by induction. However, only one step of induction is shown here, i.e.,

$$x(t = 0) \in B(w_0, z_0) = B(w, z) \Rightarrow \exists t_0 > 0 \text{ so that } x(t_0) \in B(w_1, z_1) \quad \text{(A.10-3)}$$

for if (A.10-3) is true then since $B(w_1, z_1)$ is invaraint by (A.10-1), the proof of (A.10-3) can be carried out inductively.

To prove (A.10-3), another refinement is made here. Note that

$$B(w_1, z_1) = \bigcap_{1 \leqslant j \leqslant M} B(a[j], b[j])$$

where for each $j = 1, \cdots, M$, the vertices of the hyperbox $B(a[j], b[j])$ are defined by

$$a[j] = ((w_0)_1, \cdots, (w_0)_{j-1}, (w_1)_j, (w_0)_{j+1}, \cdots, (w_0)_M)$$

$$b[j] = ((z_0)_1, \cdots, (z_0)_{j-1}, (z_1)_j, (z_0)_{j+1}, \cdots, (z_0)_M).$$

In other words, $a[j]$ and $b[j]$ are the projection of the points $w_0 = w$ and $z_0 = z$, respectively, onto the hypersurface L_j. Since $a[j] \in \mathbf{P}_\alpha$ and $b[j] \in \mathbf{N}_\alpha$, $B(a[j], b[j])$ is invariant, $\forall j$, by (A.10-1). Therefore, (A.10-3) is equivalent to the following:

$$x(t = 0) \in B(w_0, z_0) = B(w, z) \Rightarrow \text{For each } j, \exists t_j > 0 \text{ so that } x(t_j) \in B(a[j], b[j]). \quad \text{(A.10-4)}$$

Referring to the definitions of $a[j]$ and $b[j]$, (A.10-4) is the same as $(w_1)_j \leqslant x_j(t_j) \leqslant (z_1)_j$, $\forall j$. The proof shall be done by contradiction. Without loss of generality, assume that for a given j, $x_j(t) < (w_1)_j$, $\forall t \geqslant 0$. This implies that $x(t)$ stays in the hyperbox defined by

$$w_0 = ((w_0)_1, \cdots, (w_0)_{j-1}, (w_0)_j, (w_0)_{j+1}, \cdots, (w_0)_M)$$

and

$$((z_0)_1, \cdots, (z_0)_{j-1}, (w_1)_j, (z_0)_{j+1}, \cdots, (z_0)_M). \quad \text{(A.10-5)}$$

So, $dx/dt > 0$, $\forall t \geqslant 0$. Therefore, $x_j(t)$ converges to $x_j(\infty) \leqslant (w_1)_j$. (Similarly, if $x_j(t) > (z_1)_j$, $\forall t$, then $x_j(\infty) \geqslant (z_1)_j$.) It must be true that dx_j/dt gets arbitrarily close to 0 as time goes on. Observe that $a[j] = ((w_0)_1, \cdots, (w_0)_{j-1}, (w_1)_j, (w_0)_{j+1}, \cdots, (w_0)_M)$ is by definition the only point in the hyperbox defined by (A.10-5) that lies on the hypersurface $\{x: dx_j/dt = 0\}$. Therefore, $x(t)$ must get arbitrarily close to $a[j]$, which means that $x(t)$ gets inside $\mathbf{P}_\alpha$ and in doing so the trajectory converges

to α (Lemma 5). This contradicts the fact that $x_j(\infty) \leqslant (w_1)_j < \alpha_j$, the jth component of α. ◆

REFERENCES

[1] C. Barbier and J.-P. Barret, "An analysis of phenomena of voltage collapse on a transmission system," *Rev. Gen. Elect.*, pp. 672–690, Oct. 1980.

[2] A. J. Calvaer and E. Van Geert, "Quasi steady-state synchronous machine linearization around an operating point and applications," *IEEE Trans. Power App. Syst.*, vol. PAS-103, pp. 1466–1472, June 1984.

[3] F. D. Galiana, "Power flow feasibility and the voltage collapse problem," in *Proc. 23rd CDC*, Las Vegas, NV, pp. 485–487, Dec. 1984.

[4] W. R. Lachs, "Voltage collapse in EHV power systems," in *IEEE PES Winter Power Meeting*, New York, Jan. 1978.

[5] P. Kessel and H. Glavitsch, "Estimating the voltage stability regions of a power system," *IEEE Trans. Power Del.*, vol. PWRD-1, pp. 346–354, July 1986.

[6] C. C. Liu and F. F. Wu, "Steady-state voltage stability regions of power systems," *Syst. Contr. Lett.*, pp. 23–31, June 1985.

[7] S. Abe, Y. Fukunaga, A. Isono, and B. Kondo, "Power system voltage stability," *IEEE Trans. Power App. Syst.*, vol. PAS-101, pp. 3830–3840, Oct. 1982.

[8] J. Medanic, M. Ilic-Spong, and J. Christensen, "Discrete models of slow voltage dynamics for under load tap-changing transformer coordination," *IEEE Trans. Power Syst.*, vol. PWRS-2, pp. 873–882, Nov. 1987.

[9] C. C. Liu, "Analysis of a voltage collapse mechanism due to effects of on-load tap changers," in *IEEE ISCAS 1986*, vol. 3, pp. 1028–1030, May 1986.

[10] F. F. Wu and C. C. Liu, "Characterization of power system small-disturbance stability with models incorporating voltage variation," *IEEE Trans. Circuits Syst.*, vol. CAS-33, Apr. 1986.

[11] J. C. Carpentier, R. Girard, and E. Scano, "Voltage collapse proximity indicators computed from an optimal power flow," in *Proc. Power Systems Computation Conf.*, Helsinki, Finland, pp. 671–678, Sept. 1984.

[12] Y. Tamura, H. Mori, and S. Iwamoto, "Relationship between voltage instability and multiple load flow solutions in electric power systems," *IEEE Trans. Power App. Syst.*, vol. PAS-102, pp. 1115–1125, 1983.

[13] R. Fischl, L. Zaragocin, F. Mercede, and H. Yan, "Power system models for voltage collapse," in *IEEE ISCAS 1986*, pp. 1015–1018.

[14] A. Tiranuchit and R. J. Thomas, "A posturing strategy against voltage instabilities in electric power systems," presented at the 1987 IEEE Power Engineering Society Winter Meeting.

[15] H. G. Kwatny, A. K. Pasrija, and L. Y. Bahar, "Static bifurcations in electric power networks," *IEEE Trans. Circuits Syst.*, vol. CAS-33, pp. 981–991, 1986.

[16] C. L. DeMarco and A. R. Bergen, "A security measure for random load disturbances in nonlinear power system models," *IEEE Trans. Circuits Syst.*, vol. CAS-34, pp. 1011–1014, Dec. 1987.

[17] A. Costi, L. Shu, and R. A. Schlueter, "Power system voltage stability and controllability," in *IEEE ISCAS 1986*, pp. 1023–1027.

[18] M. Ilic-Spong, J. S. Thorp, and M. W. Spong, "Localized response performance of the decoupled Q–V network," *IEEE Trans. Circuits Syst.*, vol. CAS-33, pp. 316–322, Mar. 1986.

[19] F. F. Wu and S. Kumagai, "Steady-state security regions of power systems," *IEEE Trans. Circuits Syst.*, vol. CAS-29, pp. 702–711, Nov. 1982.

[20] R. Fischl, T. F. Halpin, and A. Guvenis, "The application of decision theory to contingency selection," *IEEE Trans. Circuits Syst.*, vol. CAS-29, pp. 712–723.

[21] C. C. Liu, "A new method for the construction of maximal steady-state security regions of power systems," *IEEE Trans. Power Syst.*, vol. PWRS-1, pp. 19–27, Nov. 1986.

[22] M. A. Pai, *Power System Stability*. Amsterdam, The Netherlands: North Holland, 1981.

[23] J. M. Ortega and W. C. Rheinboldt, *Iterative Solution of Nonlinear Equations in Several Variables*. New York: Academic, 1970.

[24] K. Vu, "Analysis of a voltage collapse mechanism due to instability of on-load tap-changers," M.S.E.E. thesis, Univ. of Washington, Seattle, 1987.

[25] "Long term power system dynamics," EPRI Res. Project 90-7-0, Appendix IB-6.2, June 1974.

[26] A. D. Papalexopoulos, C. F. Imparato, and F. F. Wu, "Large-scale optimal power flow: Effects of initialization, decoupling & discretization," presented at the 1988 IEEE PES Summer Meeting.

[27] P. W. Sauer, C. Rajagapolan, M. A. Pai, and A. Varghese, "Critical modes and voltage instability in power systems," in *1986 Proc. IEEE ISCAS*, pp. 1019–1022.

[28] R. J. Thomas and A. Tiranuchit, "Dynamic voltage instability," presented at the 26th CDC, Los Angeles, CA, Dec. 9–11, 1987.

✠

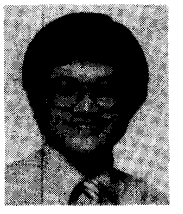

Chen-Ching Liu received the B.S.E.E. and M.S.E.E. degrees from National Taiwan University in 1976 and 1978, respectively, and the Ph.D. degree in electrical engineering and computer sciences from the University of California, Berkeley, in 1983.

He was an instructor at Army Signal and Electronics School, Taiwan, during 1978–1980. Since 1983, he has been with the Department of Electrical Engineering, University of Washington, Seattle where he is Associate Professor. In 1987, he received the Presidential Young Investigator's Award from the National Science Foundation. He is Chairman-Elect of Technical Committee on Power Systems and Power Electronics and Circuits, IEEE Circuits and Systems Society. His areas of interest are power system analysis and expert system applications.

✠

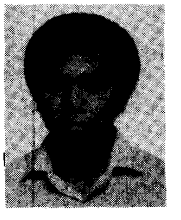

Khoi Tien Vu received the B.S.E.E. and M.S.E.E. degrees from the University of Washington, Seattle, in 1985 and 1987, respectively. While at UW, he received a Physio-Control Fellowship, a GTE Graduate Fellowship, and a Percy Halpert Memorial Fellowship. He is currently working toward the Ph.D. degree.

His interests include nonlinear system theory and its application to power systems.